

1 **Two independent proteomic approaches provide a comprehensive analysis of the synovial**
2 **fluid proteome response to Autologous Chondrocyte Implantation**

3 Charlotte H Hulme^{1,2}, Emma L Wilson^{2,3}, Heidi R Fuller¹, Sally Roberts^{1,2}, James B.
4 Richardson^{1,2}, Pete Gallacher^{1,2}, Mandy J. Peffers⁴, Sally L Shirran⁵, Catherine H. Botting⁵,
5 Karina T Wright^{1,2}

6 **Institutions:**

7 1. Institute of Science and Technology in Medicine, Keele University, Keele, Staffordshire,
8 ST5 5BG, UK

9 2. Robert Jones and Agnes Hunt Orthopaedic Hospital, Oswestry, Shropshire, SY10 7AG,
10 UK

11 3. Chester Medical School, Chester University, Chester, CH1 4BJ, UK

12 4. Institute of Ageing and Chronic Disease, University of Liverpool, Liverpool, L7 8TX, UK

13 5. BSRC Mass Spectrometry and Proteomics Facility, University of St Andrews, North
14 Haugh, Fife, KY16 9ST, UK

15
16 **Contact Details:** Charlotte H Hulme, charlotte.hulme@rjah.nhs.uk; Emma L Wilson,
17 e.wilson@chester.ac.uk; Heidi R Fuller, h.r.fuller@keele.ac.uk; Sally Roberts,
18 sally.roberts@rjah.nhs.uk; James B Richardson, james.richardson@rjah.nhs.uk; Peter
19 Gallacher, peter.gallacher@rjah.nhs.uk; Mandy J. Peffers, M.J.Peffers@liverpool.ac.uk;
20 Sally Shirran, ss101@st-andrews.ac.uk; Catherine H Blotting, cb2@st-andrews.ac.uk

21 **Correspondence:** Karina T. Wright Ph.D., ISTM, Keele University based at the RJAH
22 Orthopaedic Hospital, Oswestry, Shropshire, UK. Telephone: +44 1691 404022; e-mail:
23 Karina.Wright@rjah.nhs.uk

24

25

26

27

28

29

30

31

32

33

34

35 **Abstract**

36 **Background:** Autologous Chondrocyte Implantation (ACI) has a failure rate of approximately 20% but
37 we are yet to fully understand why. Biomarkers are needed that can pre-operatively predict which
38 patients are likely to fail, so that alternative or individualised therapies can be offered. We previously
39 used a label-free (LF) quantitation with dynamic range compression proteomic approach to assess
40 the synovial fluid (SF) of ACI responders and non-responders. However, we were only able to identify
41 a few differentially abundant proteins at baseline. Here, we build upon these previous findings by
42 assessing higher abundance proteins within these SFs, providing a more global proteome analysis
43 from which we can understand more of the biology underlying ACI success or failure.

44 **Methods:** Isobaric tagging for relative and absolute quantitation (iTRAQ) proteomics was used to
45 assess SFs from ACI responders (mean Lysholm improvement of 33; n=14) and non-responders
46 (mean Lysholm decrease of 14; n=13) at the two stages of surgery (cartilage harvest and chondrocyte
47 implantation). Differentially abundant proteins in iTRAQ and combined iTRAQ and LF datasets were
48 investigated using pathway and network analyses.

49 **Results:** iTRAQ proteomics has confirmed our previous finding that there is a marked proteome shift
50 in response to cartilage harvest (70 and 54 proteins demonstrating ≥ 2.0 fold change and $p < 0.05$
51 between Stages I and II in responders and non-responders, respectively). Further, it has highlighted
52 28 proteins that were differentially abundant between responders and non-responders to ACI, that
53 were not found in the LF study, 16 of which were altered at baseline. The differential expression of
54 two proteins (complement C1S subcomponent and matrix metalloproteinase 3 (MMP3)) was
55 confirmed biochemically. Combination of the iTRAQ and LF proteomic datasets has generated in-
56 depth SF proteome information that has been used to generate interactome networks representing
57 ACI success or failure. Functional pathways that are dysregulated in ACI non-responders have been
58 identified, including acute phase response signalling.

59 **Conclusions:** Several candidate biomarkers for baseline prediction of ACI outcome have been
60 identified. A holistic overview of the SF proteome in responders and non-responders to ACI has been
61 profiled providing a better understanding of the biological pathways underlying clinical outcome,
62 particularly the differential response to cartilage harvest in non-responders.

63 **Keywords**

64 Autologous Chondrocyte Implantation (ACI); iTRAQ proteomics; Label-free quantification proteomics;
65 Synovial Fluid; Cartilage repair; Complement C1S subcomponent; Matrix metalloproteinase 3; MMP3

66

67

68

69

70

71

72

73

74

75

76

77

78

79

80

81

82

83

84

85

86

87

88

89

90

91

92 **Background**

93 Identification of putative biomarkers that can be used to predict patient outcome prior to treatment for
94 cartilage injury has been highlighted as a key initiative for the prevention of osteoarthritis (OA) by the
95 Osteoarthritis Research Society International (OARSI) (1). Further, the recent National Institute for
96 Health and Care Excellence (NICE) recommendation for use of the cell therapy Autologous
97 Chondrocyte Implantation (ACI), in the UK National Health Service (NHS) has increased the need to
98 identify accurate prognostic biomarkers for this application (2).

99 We recently published the first study (3), to our knowledge, that has used a proteomic approach with
100 the aim of identifying candidate biomarkers to predict the success of ACI, a cellular therapy for the
101 treatment of traumatic cartilage injury (4,5). This therapy is a two-stage procedure; during the initial
102 surgery (Stage I) healthy cartilage is harvested from a minor load-bearing region of the joint, then
103 chondrocytes are isolated and culture expanded for three to four weeks prior to a second surgery in
104 which the chondrocytes are implanted into the cartilage defect (Stage II) (5,6). Approximately 500
105 patients have been treated with ACI in our centre and despite an 81% success rate (7), we are yet to
106 fully understand why some individuals fail to respond well. We have identified a biomarker,
107 aggrecanase-1, that when its activity is un-detectable pre-operatively, can be used together with
108 known demographic and injury-associated risk factors to help predict ACI success (8,9). However, we
109 are yet to identify a biomarker (or panel of biomarkers) that can be used to accurately predict ACI
110 failure. The identification of such a biomarker(s) for ACI and other cartilage repair strategies would
111 allow for the better stratification of patients' prior to joint surgery and may provide candidates for
112 therapies to improve ACI success.

113 Proteomic analyses remain one of the most widely used methods to identify novel biomarker
114 candidates and have previously been utilised to identify biomarkers of OA progression (as
115 summarised by Hsueh *et al.* in 2014 (10)). The synovial fluid (SF) provides an attractive biological
116 fluid for biomarker identification, as it bathes the injured joint and therefore contains proteins that
117 might reflect the whole joint environment. Proteomic profiling of the SF, however, is technically difficult
118 due to the broad dynamic range of proteins present within it (7,8). Several un-biased, global
119 proteomic studies for the identification of biomarkers within the SF have been completed.
120 Nevertheless, the number of protein 'hits' has been somewhat limited, as authors have tended to

121 either profile SFs with no pre-treatment to account for the wide range of proteins (11–16) or have
122 depleted high abundance proteins (17–22) meaning that the altered quantities of these proteins
123 cannot be considered.

124 Isobaric tags for absolute and relative quantitation (iTRAQ) is reported as the most accurate labelling
125 method for quantifying comparative abundance of proteins (23). When compared to label free (LF)
126 quantitation proteomics, iTRAQ quantitation has traditionally been considered as a more accurate
127 technique (24); however as mass spectrometers improve, these techniques are becoming more
128 comparable and LF quantitation is becoming increasingly popular (25). Unlike LF quantitation
129 proteomics, iTRAQ utilises isobaric tags to label the primary amines at the peptide level, prior to
130 pooling the samples to enable simultaneous identification and quantitation of the proteins. 4plex and
131 8plex labels are available enabling quantitation of up to 8 conditions in a single analysis, thus
132 minimising the number of mass spectrometry runs which can be cost effective and time efficient.
133 However, when compared to LF quantitation, in which any number of samples can be analysed and
134 compared, iTRAQ labelling limits the number of samples that can be compared, meaning biological
135 replicate samples are often pooled together into relevant biological conditions. iTRAQ proteomics is a
136 commonly used tool for the identification of biomarkers in a plethora of diseases. This proteomic
137 approach has been used to profile the SF proteome (20,26), successfully identifying differentially
138 abundant protein biomarker candidates for several diseases/conditions.

139 Our previous study highlighted the potential of using protein equalisation to study low abundance
140 proteins in human SF, but this identified few differentially abundant proteins in baseline SF, when
141 comparing individuals who did or did not do well following cartilage repair therapy (1). This study,
142 therefore, aimed to increase the number of protein biomarker candidates that could be identified for
143 the pre-operative prediction of clinical outcome following ACI and to allow for the assessment of high
144 abundance proteins which may also strengthen our understanding of the biological processes
145 underlying treatment success.

146

147

148

149 **Methods**

150 **Synovial fluid collection and storage**

151 SF was collected, as described previously (3,8,27), from the knee joints of patients, with informed
152 consent and following local research ethical approval. Immediately prior to both ACI surgeries, Stage I
153 (cartilage harvest) and Stage II (chondrocyte implantation), 20 mL of saline was injected into the joint
154 and 20 rounds of leg flexion and extension carried out to allow aspiration of as much SF as possible
155 (3,27). SF was then centrifuged at 6,000 g for 15 minutes at 4°C and split into aliquots for long-term
156 storage in liquid nitrogen. The dilution factor of the SF samples was calculated by comparing urea
157 content in SF to matched blood plasma using a QuantiChrom™ Urea Assay kit (BioAssay Systems,
158 Hayward, USA) according to manufacturer's instructions, as described previously (3,8,28) and SF
159 samples with a dilution factor greater than 10 were excluded from the study.

160 Clinical responders to ACI were defined as individuals who demonstrated an increase of at least 10
161 points in the Lysholm score at 12 months post-treatment compared to their baseline score, as has
162 been used previously (29–31). The Lysholm score is a validated (32), patient-self assessment score,
163 encompassing knee pain and joint function that ranges from 0-100, with 100 representing 'perfect'
164 knee function (32,33). Thirteen patients were considered as non-responders to ACI, demonstrating a
165 mean decrease in Lysholm score of 14 points (range -4 - -46) and 14 SF donors were considered
166 responders with a mean improvement of 33 points (range 17-54).

167 **Sample preparation and analysis using iTRAQ proteomics (iTRAQ nLC-MS/MS)**

168 Total protein was quantified using a Pierce™ 660nm protein assay (Thermo Scientific, Hemel
169 Hempstead, UK) (34) and a total of 200 µg of SF protein was pooled equally from the donors in each
170 of the following experimental groups: Stage I, responders (n=8); Stage I, non-responders (n=7); Stage
171 II responders (n=12) and Stage II, non-responders (n=12). The pooled samples were then
172 precipitated in six volumes of ice-cold acetone overnight at -20°C. The precipitates were pelleted by
173 centrifugation at 13,000 g for 10 mins at 4°C before being re-suspended in 200 µl triethylammonium
174 bicarbonate (TEAB) buffer. Eighty five micrograms of protein for each experimental sample was then
175 subjected to reduction, alkylation (as instructed in the iTRAQ labelling kit (Applied Biosystems,
176 Bleiswijk, Netherlands)). Sequencing grade modified trypsin (Promega) (10 µg per 85 µg of protein)

	Stage I		Stage II		Mann-Whitney U (p-value) (A)R v NR- SI; (B) R v NR- SI	Mann-Whitney U (p-value) (A)SI v SII-R; (B) SI v SII- NR
	Responders (n=8)	Non-responders (n=7)	Responders (n=12)	Non-responders (n=12)		
Difference in Lysholm Score	27 (17-38)	-8 (-4 - -17)	34 (17-54)	-11 (-4 - -46)	(A) 0.0003; (B) <0.0001	(A) 0.21; (B) 0.55
BMI (kg/m²)	29 (23-31)	27 (24-31)	27 (23-48)	29 (22-36)	(A) 0.94; (B) 0.54	(A) 0.73; (B) 0.68
Age (years)	32 (17-49)	40 (25-50)	40 (17-90)	43 (25-52)	(A) 0.28; (B) 0.92	(A) 0.17; (B) 0.58
Male/Female (No. of participants)	8/0	7/0	11/1	10/2	(A) >0.99; (B) >0.99	(A) >0.99; (B) 0.51
Smoker (No. of participants)	1	2	1	3	(A) 0.54; (B) 0.59	(A) >0.99; (B) >0.99
Dilution Factor of SF	5 (3-9)	4 (2-7)	4 (1-9)	3 (2-5)	(A) 0.48; (B) 0.25	(A) 0.53; (B) 0.50
Total defect area (cm²)	14 (0.4-24)	6 (0.6-12)	6 (1-20)	5 (0.6-12)	(A) 0.74; (B) 0.35	(A) 0.45; (B) 0.28
Patella defect (No. of participants)	1	1	4	2	(A) >0.99; (B) 0.64	(A) 0.60; (B) >0.99
LFC defect (No. of participants)	2	0	0	0	(A) 0.47; (B) >0.99	(A) 0.15; (B) >0.99
LTP defect (No. of participants)	1	0	0	0	(A) >0.99; (B) >0.99	(A) 0.15; (B) >0.99
MFC defect (No. of participants)	2	2	1	6	(A) >0.99; (B) 0.07	(A) 0.54; (B) 0.63
Trochlea defect (No. of participants)	0	3	2	1	(A) 0.20; (B) >0.99	(A) 0.49; (B) 0.12
Multiple defects (No. of participants)	1	0	1	1	(A) >0.99; (B) >0.99	(A) >0.99; (B) >0.99
Unknown defect location (No. of participants)	1	1	4	2	(A) >0.99; (B) 0.64	(A) 0.60; (B) >0.99

177

178 **Table 1:** Demographic data for patient samples from Stage I or Stage II were analysed, those who responded well clinically (responders) or who did not
179 respond well (non-responders) to autologous chondrocyte implantation (ACI) are indicated in separate groups. None of the demographic parameters, other
180 than a difference in Lysholm score, showed differences between responders (R) and non-responders (NR) in individuals whose SFs from Stage I (SI) or
181 Stage II (SII) were compared, nor were there differences between individuals who were either responders or non-responders when comparing Stage I and
182 Stage II samples ($p \geq 0.05$; Mann-Whitney U). Data are median (range). Abbreviations: BMI, body mass index; LFC, lateral femoral condyle; LTP, lateral tibial
183 plateau; MFC, medial femoral condyle.

184 was then added to the samples for overnight digestion at 37°C. Tryptic digests were labelled with the
185 iTRAQ tags, according to manufacturer's instructions: 114- Stage II, responders; 115- Stage II, non-
186 responders; 116- Stage I, responders; 117- Stage I, non-responders, before being pooled to one
187 microcentrifuge tube prior to being dried down in a vacuum centrifuge.

188 iTRAQ- labelled peptides were resuspended in 0.6 mL of loading Buffer Ascx (10 mM monopotassium
189 phosphate (KH₂PO₄), 20% acetonitrile (MeCN), pH 3.0), followed by sonication. The pH was adjusted
190 to 3.0 with 0.5 M orthophosphoric acid (H₃PO₄). The peptides were separated by strong cation
191 exchange chromatography as described previously (35). A total of 14 SCX fractions were analysed by
192 nanoLC ESI MSMS using a TripleTOF 5600 tandem mass spectrometer (ABSciex, Foster City, CA)
193 as described previously (36)

194 The raw mass spectrometry data file was subsequently analysed using ProteinPilot 4.5 software with
195 the Paragon™ and ProGroup™ algorithms (ABSciex) against the human sequences in the Swiss-Prot
196 database (downloaded Dec 2012). Searches were performed using the pre-set iTRAQ settings in
197 ProteinPilot. Trypsin was selected as the cleavage enzyme and MMTS for the modification of
198 cysteines with a "Thorough ID" search effort. ProteinPilot's Bias correction assumes that most
199 proteins do not change in expression. Finally, detected proteins were reported with a Protein
200 Threshold [Unused ProtScore (confidence)] >0.05 and used in the quantitative analysis if they were
201 identified with two or more unique peptides with 95% confidence or above. P-values and false
202 discovery rates for the iTRAQ ratios were calculated by the ProteinPilot software. Proteins with iTRAQ
203 ratios with p-values ≤0.05 and with differential abundances of ≥±2.0 fold change (FC) were used in
204 further analysis.

205 **Verification of iTRAQ nLC-MS/MS results using Enzyme Linked Immunosorbant Assay (ELISA)**

206 Two proteins of biological relevance were measured by ELISA in the non-pooled samples to verify the
207 mass -spectrometry findings. Firstly, Complement C1S subcomponent (C1s) was selected, as this
208 protein demonstrated differential abundance between responders and non-responders to ACI within
209 the baseline SF (prior to Stage I surgery) and, therefore, could have potential as a biomarker of
210 outcome prediction. C1s was assessed using a human ELISA (Cusabio, USA). Samples were first
211 assayed using a 1 in 100 dilution in assay sample diluent and for those samples that were
212 undetectable in the assay was repeated using undiluted samples. Secondly Matrix metalloproteinase

213 3 (MMP3) was selected to investigate the differential response to Stage I surgery (i.e. the proteome
214 shift between Stages I and II) in non-responders to ACI. MMP3 was assessed using a human
215 Quantikine[®] ELISA (R&D Systems, Abingdon, UK). Samples were diluted 1 in 100 in assay kit diluent
216 prior to assessment. Both ELISAs were carried out according to the manufacturer's instructions and
217 protein concentrations were normalised to the sample dilution factor. Statistical analysis was
218 performed in GraphPad Prism version 6.0. Student's t-tests were used to assess differential
219 abundance.

220 **Assessment of the overlap of proteins identified from the two proteomic approaches**

221 In order to assess whether the use of two independent proteomic approaches allows for a greater
222 number of significant protein changes to be identified, the datasets from this study (iTRAQ nLC-
223 MS/MS) and our previously published study assessing the same patient samples (LF LC-MS/MS; (3))
224 were compared to one another. Venn-diagrams were plotted using VENNY 2.1.0 software (37), to
225 assess the overlap of differentially abundant proteins that was identified via the two approaches.

226 **Pathway and network analysis of proteomic datasets**

227 The datasets generated from both proteomic approaches were combined. Specifically, proteins which
228 were differentially expressed (≥ 1.2 FC; $p \leq 0.05$) in each biological comparison e.g. Stage I responders
229 versus non-responders, in either proteomic approach were merged into a single dataset. A modest
230 fold-change cut-off was used to ensure the greatest number of differentially abundant proteins could
231 be included in the pathway and network analyses, as has been used previously (3,18). The iTRAQ
232 nLC-MS/MS dataset independently and when merged with the LF dataset was analysed using
233 pathway enrichment analysis (Ingenuity, Qiagen, US) to identify and visualise affected canonical
234 pathways. Pathways with $p \leq 0.005$ were considered as statistically significant (Fisher's exact test).

235 The merged LF & iTRAQ nLC-MS/MS datasets of proteomic response to cartilage harvest (e.g.
236 differential abundance between Stages I and II) in responders and non-responders were assessed
237 using interactome network analysis, which is an unbiased mathematical method of visualising and
238 interpreting complex interactions between large numbers of molecules (38). Interactome networks are
239 made up of nodes (the individual objects being studied, e.g. proteins) and edges (the connections
240 between the objects, e.g. known protein-protein interactions) (39). By studying groups of proteins that

241 are highly interconnected, known as modules, key functions within an interactome network can be
242 highlighted (39). Conducting interactome network analysis alongside pathway enrichment analysis,
243 allows for greater confidence in the selection of candidate pathways or molecules for further study as
244 these represent two independent methods of mapping the data, known protein-protein interactions
245 and text mining, respectively. The interactions between the differentially abundant proteins were
246 assessed using the Protein Interaction Network Analysis For Multiple Sets (PINA4MS) app (40) in
247 Cytoscape (v3.0) to generate network models based on protein-protein interactions. These models
248 were either based upon only those proteins identified in the proteomic analyses (non-inferred nodes)
249 or from proteins identified in the proteomic analyses alongside their inferred interactions (inferred
250 nodes) (41). The Moduland (v2.8.3) algorithm (42) was applied to the interactome networks in
251 Cytoscape (v3.0) to identify highly connected clusters of proteins (modules) that demarcate the
252 hierarchical structure of the interactome network. The biological function of each module was
253 assessed by analysing the proteins identified within each module using the pathway analysis tool in
254 Reactome software (43,44). The significance of the pathway functions identified in Reactome was
255 determined by Fisher's exact test and $p \leq 0.05$ was considered statistically significant.

256

257

258

259

260

261

262

263

264

265

266 **Results**

267 Proteomic data has been deposited in the PRIDE ProteomeXchange and can be accessed using the
268 identifier PXD008321.

269 **Identification of proteins to predict ACI outcome prior to Stage I or Stage II**

270 iTRAQ nLC-MS/MS highlighted 16 proteins ($\geq \pm 2.0$ FC; $p \leq 0.05$) which were differentially abundant
271 between responders and non-responders to ACI at baseline (immediately prior to Stage I) (Table 2).
272 Prior to Stage II of the ACI procedure, 12 proteins displayed differential abundance between
273 responders and non-responders (Table 3).

274 At both stages of treatment, SF analysed using iTRAQ nLC-MS/MS identified a greater number of
275 differentially abundant proteins between individuals who did or did not respond well to ACI compared
276 to SF which had undergone protein normalisation using ProteoMiner™ beads and LF LC-MS/MS
277 analysis (3). Further, the two proteomic techniques identified no common differentially abundant
278 proteins.

279 **Differential abundance of proteins a Stage II compared to Stage I of ACI**

280 Proteomic profiling of the SF using iTRAQ nLC-MS/MS highlighted a considerable effect of the
281 cartilage harvest procedure (Stage I) in both responders and non-responders, with 70 and 54 proteins
282 being differentially abundant between Stages I and II, respectively. Thus strengthening the similar
283 findings from the analysis of these samples using LF LC-MS/MS (3).

284 Interestingly, the iTRAQ nLC-MS/MS and LF LC-MS/MS identified no common Stage I compared to
285 Stage II protein differences in the clinical responders (70 differentially abundant proteins identified by
286 iTRAQ nLC-MS/MS and 14 identified by LF LC-MS/MS; Table 4). This lack of overlap between the
287 two proteomic techniques is highlighted in Figure 1. There were, however, six proteins (gelsolin,
288 vitamin K-dependent protein S, C4b binding protein alpha chain, fibrinogen alpha chain, fibrinogen
289 beta chain and fibrinogen gamma chain) that were identified by both proteomic techniques in the non-
290 responders, all of which showed commonality in the direction of protein shift, across the MS platforms,
291 with iTRAQ nLC-MS/MS consistently resulting in greater differences in abundance than those
292 identified from the LF LC-MS/MS data. A total of 54 protein abundance changes between Stages I
293 and II in non-responders were identified using iTRAQ nLC-MS/MS and 55 protein differences were

Protein		Fold Change	Identified using:	
Description	Accession		LF LC-MS/MS	iTRAQ nLC-MS/MS
Complement C1s subcomponent	P09871	-5.15		+
Haptoglobin	P00738	-4.49		+
Mesencephalic astrocyte-derived neurotrophic factor	P55145	2.15		+
Plasma protease C1 inhibitor	P05155	2.19		+
Ig kappa chain V-II region MIL	P01615	2.60	+	
Bifunctional glutamate/proline--tRNA ligase	P07814	2.61		+
Pigment epithelium-derived factor	P36955	3.13		+
Apolipoprotein A-IV	P06727	3.19		+
Apolipoprotein L1	O14791	3.19		+
N-acetylglucosamine-6-sulfatase	P15586	3.25		+
Retinol-binding protein 4	P02753	3.34		+
Inter-alpha-trypsin inhibitor heavy chain H1	P19827	3.37		+
Extracellular matrix protein 1	Q16610	3.77		+
Lumican	P51884	3.80		+
Histidine-rich glycoprotein	P04196	3.84		+
Endoplasmin	P14625	4.37		+
Serum paraoxonase/arylesterase 1	P27169	4.41		+

294

295 **Table 2:** Fold change of proteins that are differentially abundant ($\geq \pm 2.0$ FC; $p \leq 0.05$; protein identified
296 by at least 2 unique peptides) in the synovial fluid of clinical non-responders compared to clinical
297 responders to ACI immediately prior to Stage I. Positive numbers denote higher abundance in non-
298 responders compared to responders. Proteins were identified using either protein dynamic
299 compression coupled with label free quantification liquid-chromatography tandem mass spectrometry
300 (LF LC-MS/MS) or no protein dynamic compression with isobaric tags for absolute and relative
301 quantitation (iTRAQ) LC-MS/MS.

302

303

304

305

306

307

308

309

310

311

Protein		Fold Change	Identified using:	
Description	Accession		LF LC-MS/MS	iTRAQ nLC-MS/MS
40S ribosomal protein S14	P62263	-8.63		+
Kinectin	Q86UP2	-6.20		+
Apolipoprotein C-III	P02656	-2.78		+
High mobility group protein B1	P09429	-2.56		+
Kininogen-1	P01042	2.27		+
26S protease regulatory subunit 7	P35998	2.34	+	
26S proteasome non-ATPase regulatory subunit 13	Q9UNM6	2.43	+	
Alpha-enolase	P06733	2.56		+
Alpha-2-HS-glycoprotein	P02765	2.78		+
Hemopexin	P02790	2.88		+
Ferritin light chain	P02792	2.91	+	
Platelet factor 4	P02776	3.26	+	
Thrombospondin-1	P07996	3.40	+	
Nucleosome assembly protein 1-like 1	P55209	4.94	+	
Cofilin-1	P23528	7.08	+	
EH domain-containing protein 1	Q9H4M9	7.30	+	
Hemoglobin subunit delta	P02042	8.09		+
Protein S100-A6	P06703	8.39		+
T-complex protein 1 subunit eta	Q99832	8.43	+	
Hemoglobin subunit beta	P68871	32.81		+
Hemoglobin subunit alpha	P69905	44.06		+

312

313 **Table 3:** Fold change of proteins that are differentially abundant ($\geq \pm 2.0$ FC; $p \leq 0.05$; protein identified
314 by at least 2 unique peptides) in the synovial fluid of clinical non-responders compared to clinical
315 responders to ACI immediately prior to Stage II. Positive numbers denote higher abundance in non-
316 responders compared to responders. Proteins were identified using either protein dynamic
317 compression coupled with label free quantification liquid-chromatography tandem mass spectrometry
318 (LF LC-MS/MS) or no protein dynamic compression with isobaric tags for absolute and relative
319 quantitation (iTRAQ) LC-MS/MS.

320

321

322

323

324

325

326

327

Protein		Fold Change	Identified using:	
Description	Accession		LF LC-MS/MS	iTRAQ nLC-MS/MS
Microtubule-associated protein 1B	P46821	-20.65	+	
40S ribosomal protein S14	P62263	-16.75		+
Protein disulfide-isomerase A6	Q15084	-7.59		+
Nucleolin	P19338	-5.11		+
Histone H1.2	P16403	-3.84		+
Stress-induced-phosphoprotein 1	P31948	-3.63		+
Complement factor D	P00746	-3.44		+
SH3 domain-binding glutamic acid-rich-like protein	O75368	-3.44		+
Heterogeneous nuclear ribonucleoprotein U	Q00839	-3.40		+
78 kDa glucose-regulated protein	P11021	-3.25		+
Cartilage oligomeric matrix protein	P49747	-3.10		+
Annexin A2	P07335	-2.96		+
Mesencephalic astrocyte-derived neurotrophic factor	P55145	-2.86		+
Kinectin	Q86UP2	-2.81		+
Complement factor H-related protein 3	Q02985	-2.77	+	
Phosphatidylethanolamine-binding protein 1	P30086	-2.51		+
Peroxiredoxin-4	Q13162	-2.49	+	
Regucalcin	Q15493	-2.44		+
Malate dehydrogenase, mitochondrial	P40926	-2.44		+
N-acetylglucosamine-6-sulfatase	P15586	-2.31		+
Gelsolin	P06396	-2.27		+
Alpha-endosulfine	O43768	-2.25		+
Peptidyl-prolyl cis-trans isomerase FKBP3	Q00688	-2.11		+
Hemopexin	P02790	2.05		+
Serum paraoxonase/arylesterase 1	P27169	2.07		+
Secreted phosphoprotein 24	Q13103	2.10	+	
Heparin cofactor 2	P05546	2.13		+
Ferritin light chain	P02792	2.21	+	
Attractin	O75882	2.21		+
Ig gamma-2 chain C region	P01859	2.23		+
Plasma kallikrein	P03952	2.24		+
Chondroitin sulfate proteoglycan 4	Q6UVK1	2.35	+	
Collagen alpha-2(I) chain	P08123	2.37	+	
Collagen alpha-1(V) chain	P20908	2.54	+	
CD5 antigen-like	O43866	2.58		+
Phospholipid transfer protein	P55058	2.63		+
Insulin-like growth factor-binding protein complex acid labile subunit	P35858	2.68		+
Prothrombin	P00734	2.68		+
Beta-2-glycoprotein 1	P02749	2.78		+
Collagen alpha-2(V) chain	P05997	2.84	+	
Plasma protease C1 inhibitor	P05155	2.91		+

Serum amyloid P-component	P02743	2.91		+
Complement C1q subcomponent subunit B	P02746	3.01		+
Collagen alpha-1(I) chain	P02452	3.05	+	
Alpha-2-antiplasmin	P08697	3.10		+
Alpha-1B-glycoprotein	P04217	3.19		+
Complement factor B	P00751	3.25		+
Complement component C7	P10643	3.40		+
Vitamin K-dependent protein S	P07225	3.42		+
Apolipoprotein E	P02649	3.44		+
Alpha-1-antichymotrypsin	P01011	3.44		+
Carboxypeptidase N subunit 2	P22792	3.53		+
Vitronectin	P04004	3.63		+
Inter-alpha-trypsin inhibitor heavy chain H3	Q06033	3.66		+
Complement C5 O	P01031	4.00		+
Plasminogen	P00747	4.06		+
Kininogen-1	P01042	4.17		+
Platelet factor 4	P02776	4.26	+	
Inter-alpha-trypsin inhibitor heavy chain H2	P19823	4.49		+
Periostin	Q15063	4.57	+	
Apolipoprotein L1	O14791	4.61		+
Protein 4.1	P11171	4.66	+	
26S proteasome non-ATPase regulatory subunit 13	Q9UNM6	4.78	+	
Inter-alpha-trypsin inhibitor heavy chain H1	P19827	5.01		+
Inter-alpha-trypsin inhibitor heavy chain H4	Q14624	5.06		+
Complement C1r subcomponent	P00736	5.15		+
Complement component C6	P13671	5.45		+
Complement factor H	P08603	5.50		+
Catalase	P04040	5.60		+
Ficolin-3	O75636	6.43		+
C4b-binding protein alpha chain	P04003	7.05		+
Ceruloplasmin	P00450	7.51		+
Pregnancy zone protein	P20742	8.09		+
Fibrinogen alpha chain	P02671	8.40		+
Apolipoprotein M	O95445	9.04		+
Protein S100-A6	P06703	9.82		+
Hemoglobin subunit alpha	P69905	9.82		+
Complement C1s subcomponent	P09871	10.00		+
Ig mu chain C region	P01871	12.13		+
Haptoglobin	P00738	13.68		+
Fibrinogen beta chain	P02675	16.90		+
Hemoglobin subunit beta	P68871	19.41		+
Fibrinogen gamma chain	P02679	23.55		+

328 **Table 4:** Fold change of proteins that are differentially abundant ($\geq \pm 2.0$ FC; $p \leq 0.05$; protein identified
329 by at least 2 unique peptides) in the synovial fluid of clinical responders at Stage II compared to Stage

330 I of ACI. Positive numbers denote higher abundance at Stage II compared to Stage I. Proteins were
331 identified using either protein dynamic compression coupled with label free quantification liquid-
332 chromatography tandem mass spectrometry (LF LC-MS/MS) or no protein dynamic compression with
333 isobaric tags for absolute and relative quantitation (iTRAQ) LC-MS/MS.

334

335

336

337

338

339

340

341

342

343

344

345

346

347

348

349

350

351

352

353

354

355

356

357 identified by LF LC-MS/MS (Table 5; Figure 1).

358 **iTRAQ nLC-MS/MS confirmed that there is a significant response to the cartilage harvest**
359 **procedure (Stage I) in non-responders to ACI**

360 Pathway analysis of the iTRAQ nLC-MS/MS identified proteins, using the pathway enrichment tools in
361 Ingenuity, suggested that the proteins which were differentially abundant at Stage II compared to
362 Stage I in non-responders are likely to impact on numerous canonical pathways; many of which were
363 confirmatory of the previously published functional pathways identified from the LF nLC-MS/MS
364 derived proteins (3). These functional pathways included acute phase response signalling ($p=2.93$
365 $\times 10^{-1}$), the complement system ($p=2.11 \times 10^{-1}$) and Liver X receptor/ Retinoic X receptor (LXR/RXR)
366 signalling ($p=1.95 \times 10^{-1}$). Moreover, many more functional pathways were affected as a result of the
367 proteins that were differentially abundant in response to Stage II compared to Stage I in non-
368 responders compared to responders (Supplementary Tables 1 and 2); reiterating that the SF
369 proteome response to cartilage harvest is more distinct in non-responders to ACI.

370 **Similar pathways were identified from the differentially abundant proteins identified by the**
371 **iTRAQ nLC-MS/MS and LF LC-MS/MS analyses**

372 Both iTRAQ nLC-MS/MS and LF LC-MS/MS analyses resulted in the acute phase response signalling
373 being highlighted as one of the most significantly affected pathways in response to cartilage harvest in
374 non-responders to ACI, therefore this pathway was further assessed. Figure 4 highlights that analysis
375 of the SF proteome using the two independent proteomic techniques resulted in a greater number of
376 differentially abundant downstream proteins being identified. In addition, many complementary
377 proteins have been identified when comparing these datasets, with the vast majority of proteins that
378 are predicted to be increased in the plasma (the standard bodily fluid referred to in Ingenuity) during
379 the acute phase response being more abundant in the SF at Stage II compared to Stage I and vice
380 versa.

381 As the results of the two proteomic approaches seem to be complementary to one another, the two
382 datasets were combined to generate a more comprehensive profile of the SF proteome. Pathway
383 analysis using Ingenuity again identified many similar functional pathways as were identified via the
384 independent LF LC-MS/MS and iTRAQ nLC-MS/MS datasets. The most significant canonical

Protein		Fold Change	Identified using:	
Description	Accession		LF LC-MS/MS	iTRAQ nLC-MS/MS
Protein S100-A6	P06703	-4.49		+
Annexin A1	P04083	-4.13		+
Hemoglobin subunit beta	P68871	-4.09		+
Complement factor D	P00746	-3.87		+
Perilipin-4	Q96Q06	-3.87	+	
<i>Gelsolin</i>	<i>P06396</i>	-3.31		+
<i>Gelsolin</i>	<i>P06396</i>	-1.68	+	
Syntaxin-7	O15400	-3.31	+	
Fermitin family homolog 3	Q86UX7	-3.29	+	
Histone H1.2	P16403	-3.13		+
Transaldolase	P37837	-3.08		+
Neuroblast differentiation-associated protein AHNAK	Q09666	-2.78	+	
Heterogeneous nuclear ribonucleoprotein K	P61978	-2.69	+	
Hyaluronan and proteoglycan link protein 3	Q96S86	-2.65	+	
Alpha-enolase	P06733	-2.63		+
ATP-citrate synthase	P53396	-2.63	+	
Annexin A2	P07355	-2.56		+
Fatty acid-binding protein, epidermal	Q01469	-2.43	+	
Peroxiredoxin-1	Q06830	-2.20	+	
Tripeptidyl-peptidase 1	O14773	-2.19	+	
Insulin-like growth factor-binding protein 6	P24592	-2.13	+	
Na(+)/H(+) exchange regulatory cofactor NHE-RF1	O14745	-2.11	+	
Peroxiredoxin-6	P30041	-2.08	+	
Histamine N-methyltransferase	P50135	-2.07	+	
Mortality factor 4-like protein 1	Q9UBU8	-2.06	+	
Transcription elongation factor A protein 1	P23193	-2.06	+	
Cartilage acidic protein 1	Q9NQ79	-2.03		+
2',3'-cyclic-nucleotide 3'-phosphodiesterase	P09543	-1.20	+	
Fructose-bisphosphate aldolase A	P04075	-1.97	+	
Leucine zipper transcription factor-like protein 1	Q9NQ48	-1.94	+	
Protein S100-A13	Q99584	-1.94	+	
40S ribosomal protein S3	P23396	-1.93	+	
Filamin-A	P21333	-1.92	+	
Microtubule-associated protein RP/EB family member 1	Q15691	-1.92	+	
Nuclear migration protein nudC	Q9Y266	-1.90	+	
Prostaglandin E synthase 3	Q15185	-1.85	+	
Stress-induced-phosphoprotein 1	P31948	-1.85	+	
Cytokine-like protein 1	Q9NRR1	-1.81	+	
Plastin-2	P13796	-1.81	+	
Coronin-1C	Q9ULV4	-1.80	+	
Vinculin	P18206	-1.80	+	

Cathepsin K	P43235	-1.79	+	
Hsc70-interacting protein	P50502;Q8IZP2	-1.76	+	
Putative phospholipase B-like 2	Q8NHP8	-1.74	+	
Spectrin beta chain, erythrocytic	P11277	-1.73	+	
Complement factor I	P05156	2.11		+
Alpha-1-antichymotrypsin	P01011	2.22		+
Titin	Q8WZ42	2.23		+
Cytoplasmic dynein 1 heavy chain 1	Q14204	2.23	+	
F-actin-capping protein subunit beta	P47756	2.25	+	
Mannan-binding lectin serine protease 1	P48740	2.26	+	
Serum amyloid P-component	P02743	2.27		+
Complement component C6	P13671	2.29		+
Thrombospondin-3	P49746	2.36	+	
Soluble scavenger receptor cysteine-rich domain-containing protein SSC5D	A1L4H1	2.39	+	
Plasma kallikrein	P03952	2.42		+
Complement factor B	P00751	2.47		+
Afamin	P43652	2.47		+
<u>Vitamin K-dependent protein S</u>	P07225	2.49	+	
<u>Vitamin K-dependent protein S</u>	P07225	3.08		+
Integrin beta-like protein 1	O95965	2.51	+	
C4b-binding protein beta chain	P20851	2.55	+	
Fibronectin	P02751	2.58	+	
Clusterin	P10909	2.65		+
Vitronectin	P04004	2.68		+
Bifunctional glutamate/proline--tRNA ligase	P07814	2.70		+
Nucleobindin-1	Q02818	2.71	+	
Complement component C9	P02748	2.75		+
Zinc-alpha-2-glycoprotein	P25311	2.75		+
Complement C1r subcomponent	P00736	2.83		+
Heparin cofactor 2	P05546	2.83		+
Ferritin light chain	P02792	2.84	+	
Proteoglycan 4	Q92954	2.88		+
<u>C4b-binding protein alpha chain</u>	P04003	2.91	+	
<u>C4b-binding protein alpha chain</u>	P04003	10.38		+
<i>Matrix Metalloproteinase 3</i>	P08254	2.91		+
Attractin	O75882	2.94		+
Insulin-like growth factor-binding protein complex acid labile subunit	P35858	3.02		+
Alpha-1B-glycoprotein	P04217	3.05		+
<u>Fibrinogen alpha chain</u>	P02671	3.10	+	
<u>Fibrinogen alpha chain</u>	P02671	11.91		+
Lumican	P51884	3.13		+
Chondroitin sulfate proteoglycan 4	Q6UVK1	3.16	+	
Collagen alpha-2(V) chain	P05997	3.19	+	

Complement C2	P06681	3.22		+
<i>Fibrinogen beta chain</i>	P02675	3.25	+	
<i>Fibrinogen beta chain</i>	P02675	18.37		+
Secreted phosphoprotein 24	Q13103	3.26	+	
Matrix Metalloproteinase 1	P03956	3.33	+	
Latent-transforming growth factor beta-binding protein 1	Q14766	3.45	+	
Phospholipid transfer protein	P55058	3.47		+
Inter-alpha-trypsin inhibitor heavy chain H3	Q06033	3.47		+
Complement C1q tumor necrosis factor-related protein 3	Q9BXJ4	3.50	+	
Adipocyte enhancer-binding protein 1	Q8IUX7;Q8N436	3.51	+	
Adiponectin	Q15848	3.52	+	
<i>Fibrinogen gamma chain</i>	P02679	3.79	+	
<i>Fibrinogen gamma chain</i>	P02679	18.37		+
Plasminogen	P00747	3.84		+
Apolipoprotein C-II	P02655	3.94		+
CD5 antigen-like	O43866	4.17		+
Collagen alpha-1(V) chain	P20908	4.26	+	
Complement factor H	P08603	4.57		+
Inter-alpha-trypsin inhibitor heavy chain H4	Q14624	4.61		+
Complement C5	P01031	4.74		+
Collagen alpha-1(I) chain	P02452	4.84	+	
Ceruloplasmin	P00450	5.01		+
Histidine-rich glycoprotein	P04196	5.11		+
Target of Nesh-SH3	Q7Z7G0	5.25		+
Plasma protease C1 inhibitor	P05155	5.30		+
Apolipoprotein M	O95445	5.65		+
Inter-alpha-trypsin inhibitor heavy chain H2	P19823	5.70		+
Periostin	Q15063	5.81	+	
Apolipoprotein C-III	P02656	5.92		+
Kinectin	Q86UP2	6.02		+
Carboxypeptidase N subunit 2	P22792	7.73		+
Serum paraoxonase/arylesterase 1	P27169	8.02		+
Apolipoprotein L1	O14791	8.95		+
Ig mu chain C region	P01871	13.30		+
Apolipoprotein E	P02649	13.80		+
Inter-alpha-trypsin inhibitor heavy chain H1	P19827	15.56		+

385 **Table 5:** Fold change of proteins that are differentially abundant ($\geq \pm 2.0$ FC; $p \leq 0.05$; protein identified
386 by at least 2 unique peptides) in the synovial fluid of clinical non-responders at Stage II compared to
387 Stage I. Positive numbers denote higher abundance at Stage II compared to Stage I of ACI. Proteins
388 were identified using either protein dynamic compression coupled with label free quantification liquid-
389 chromatography tandem mass spectrometry (LF LC-MS/MS) or no protein dynamic compression with
390 isobaric tags for absolute and relative quantitation (iTRAQ) LC-MS/MS. Proteins identified by both
391 proteomic techniques are underlined and in italics.

392 pathways associated with the non-responder response to cartilage harvest (Stage II vs Stage I) were,
393 acute phase response signalling ($p=1.10 \times 10^{-9}$), intrinsic prothrombin activation pathway ($p= 3.43 \times 10^{-7}$)
394 and the complement system ($p=1.22 \times 10^{-6}$). Further, analysis of upstream regulators to these
395 dysregulated proteins included those identified using the LF LC-MS/MS analysis data alone e.g.
396 transforming growth factor beta 1 (TGFB1; $p=2.05 \times 10^{-13}$), dihydrotestosterone ($p= 4.48 \times 10^{-11}$) and
397 peroxisome proliferator-activated receptor alpha (PPARA; $p=1.09 \times 10^{-9}$) (3).

398 The combined datasets were then used to generate unbiased interactome networks that represent the
399 differentially abundant proteins (non-inferred networks), their likely interacting proteins (inferred
400 networks) and how these proteins interact with one another, resulting in models of systemic protein
401 response to cartilage harvest in either the responders or non-responders to ACI. Based on proteins
402 that were differentially abundant between Stages I and II of ACI in non-responders, an interactome
403 network consisting of 115 nodes (proteins) and 40 edges (protein-protein interactions) was generated.
404 Further, an inferred network consisting of 2893 proteins and 35576 protein-protein interactions was
405 generated based upon the addition of proteins that are likely to interact with the differentially abundant
406 proteins (PINA4MS interactome database). Proteins that were differentially abundant in response to
407 cartilage harvest in responders to ACI were used to generate interactome networks (non-inferred: 83
408 nodes and 118 edges; inferred: 2084 nodes and 54007 edges). The ModuLand algorithm was applied
409 to each of these networks to identify modules within the network that can be hierarchically ranked to
410 identify groups of proteins that are the most fundamental in the functioning of the network. Figure 4
411 highlights the top 10 modules from each of the networks generated. These modules again highlight
412 the disparity between the ACI responder and non-responder response to cartilage harvest, with only
413 modules centred on the proto-oncogene tyrosine-protein kinase (SRC) protein being identified in the
414 inferred networks of both non-responder and responder groups. Interestingly, assessment of the
415 functional pathways related to the ModuLand identified modules in the non-responder networks again
416 highlighted regulation of the complement cascade ($p= 1.68 \times 10^{-8}$; Fisher's Exact test), thus providing
417 confidence in its importance based on identification via two independent bioinformatic approaches.

418

419

420

421 **Discussion**

422 The recent NICE technology appraisal of ACI has recommended this treatment for a specific subset of
423 patients with cartilage injury in the knee (2). The identification of novel biomarkers that can strengthen
424 current patient demographic risk factors in predicting clinical outcomes (9), as well as developing a
425 greater understanding of the underlying biology associated with success and failure will be beneficial,
426 particularly as this treatment option is likely to be implemented on a wider scale in the near future.
427 This study has built upon our previously published work (3,8), highlighting a number of novel protein
428 candidates that have potential as biomarkers to predict ACI outcome. Moreover, comprehensive
429 proteomic profiling of SF has further highlighted proteome differences between responders and non-
430 responders to ACI.

431 In the majority of studies in which the SF proteome has been profiled, either high (11–16) or low (17–
432 22) abundance proteins have been assessed via depletion or non-depletion of abundant proteins prior
433 to proteomic analysis. Our study highlights that the use of both a proteome dynamic range
434 compression technique (Proteominer™) (3) in tandem with analysis of non-depleted SF samples can
435 provide a more holistic overview of proteome changes; since both iTRAQ nLC-MS/MS and LF LC-
436 MS/MS highlighted large numbers of differentially abundant proteins between Stages I and II of ACI,
437 with little crossover between techniques. This type of all-inclusive approach to unbiased whole-
438 proteome analysis of biological fluids may therefore be more successful in the identification of
439 candidate biomarkers for other treatments/ disease states beyond those investigated here.

440 A limitation of our previous study (3) was that very few proteins were identified as differentially
441 abundant between responders and non-responders at baseline. In order for biomarkers aimed at
442 predicting ACI success to be most useful clinically, patients who are likely to fail or respond to this
443 procedure need to be identified prior to any surgical intervention. Interestingly, analysis of non-
444 dynamic range compressed proteins with iTRAQ nLC-MS/MS analysis was able to detect a greater
445 number of differentially abundant proteins between responders and non-responders prior to Stage I
446 surgery. The protein with most altered abundance in responders compared to non-responders at
447 Stage I was C1s. This higher abundance in responders was confirmed in individual patient samples
448 using a biochemical assay. C1s is a major constituent of the trimeric complement C1 protein, which
449 triggers the classical complement pathway. Once activated, the classical complement pathway

450 promotes inflammation to enable the removal of damaged cells and/or microbes. Moreover, C1s has
451 been shown to cleave insulin growth factor 1 (IGF-1) (45) and insulin like growth factor binding protein
452 5 (IGFBP-5) (46). Both IGF-1 and IGFBP-5 are chondroprotective when in their intact state (45,47)
453 and inhibition of C1s activity within the canine SF reduced cleavage of IGFBP-5 and IGF-1, resulting
454 in reduced cartilage damage following anterior cruciate ligament rupture (45). These studies indicate
455 that high C1s activity levels are likely detrimental to cartilage repair. ~~In future studies, it would~~
456 ~~therefore be interesting to consider the activation state of C1s, alongside its overall abundance to~~
457 ~~determine how this protein might contribute to ACI success or failure.~~ Further, the complement
458 cascade is known to be important in the pathogenesis of OA, with OA patients demonstrating
459 increased gene expression of complement agonists compared to inhibitors (48). OA related
460 pathogenesis, such as the release of cartilage extracellular matrix molecules and the production of
461 inflammatory mediators all induce complement activation (48). The increased pre-operative levels that
462 we have identified in individuals who responded well to ACI, perhaps indicate that ACI has potential to
463 be successful in individuals who may have developed an early OA phenotype.

464 ~~It must be noted that a limitation of the iTRAQ nLC-MS/MS analysis performed in this study is that~~
465 ~~pooled samples were analysed. Pooling of the samples may have resulted in some differentially~~
466 ~~abundant proteins not being detected, particularly if there was large variation between patients for~~
467 ~~some proteins. This again highlights the benefit of performing independent pooled and non-pooled~~
468 ~~proteomic techniques to optimise the number of differentially abundant proteins that can be identified.~~
469 ~~To perform an iTRAQ proteomics study, however, the number of samples that can be individually~~
470 ~~analysed by mass spectrometry is limited by the number of available isobaric tags; currently a~~
471 ~~maximum of 8 are commercially available. Therefore, it was decided that in order to assess~~
472 ~~differences across the experimental groups, replicates of human samples were best pooled to ensure~~
473 ~~protein differences represented the complexity of human variation. Further, C1s and MMP3 were~~
474 ~~validated in individual patient SFs by biochemical means, both of which demonstrated differential~~
475 ~~abundance in the same direction of change as identified using iTRAQ proteomics. The magnitude of~~
476 ~~differential abundance, however, was lower when assessed using ELISA compared to iTRAQ nLC-~~
477 ~~MS/MS, thus highlighting the importance of biochemical validation of candidate biomarkers identified~~
478 ~~by iTRAQ nLC-MS/MS in individual technical replicate samples, particularly when considering small~~
479 ~~fold change differences from pooled samples.~~

480 Analysis of the iTRAQ nLC-MS/MS and LF LC-MS/MS datasets, both independently and when
481 combined, has highlighted that there is a marked proteome shift in response to cartilage harvest, i.e.
482 between Stages I and II of ACI. This analysis has resulted in a plethora of candidate biomarkers that
483 may have the potential to inform as to whether an individual is likely to respond well to ACI prior to
484 chondrocytes being implanted during Stage II. The proteoglycan, collagen II, IX and X degrading
485 enzyme, MMP3 (49) has been biochemically validated as one of these candidate proteins that is
486 significantly increased at Stage II compared to Stage I only in non-responders to ACI. ~~If we can~~
487 ~~identify accurate Use of these~~ biomarkers ~~these will~~could have the potential to prevent the burden of a
488 second surgery in a patient for whom this therapy is likely to be unsuccessful, ~~or~~ could indicate that a
489 greater period of time should be left from when the cartilage harvest procedure takes place and when
490 the cells are implanted ~~or that a tailored cartilage implantation procedure would be more efficacious.~~
491 ~~Alternatively, these candidate biomarkers could be used to determine whether a tailored cartilage~~
492 ~~implantation procedure would be more efficacious, for example alongside the use of anti-inflammatory~~
493 ~~drugs, molecule specific inhibitors or perhaps via the use of other cells such as mesenchymal stromal~~
494 ~~cells (MSCs) which have anti-inflammatory and immunomodulatory properties and have been shown~~
495 ~~to enhance the repair of cartilage defects (50,51).~~

496 To investigate the significant proteome shift that exists in response to cartilage harvest, pathway
497 analyses were performed to better distinguish the underlying biological mechanisms which dictate if
498 an individual will respond to ACI or not. ~~Interestingly, the number of biological pathways and functions~~
499 ~~that were differentially regulated at Stage II compared to Stage I was greater in the non-responders,~~
500 ~~again strengthening our previous findings that there is a marked and distinct proteome response to~~
501 ~~cartilage harvest in non-responders to ACI (3).~~ The acute phase response was the pathway predicted
502 to be most significantly differentially regulated in response to cartilage harvest in non-responders to
503 ACI. In-depth assessment of individual protein changes within this pathway again highlighted the
504 benefit of using independent proteomic techniques to profile the SF, as a large number of proteins
505 were differentially abundant between Stages I and II, only three of which were identified using both
506 techniques. The acute phase response is the body's first systemic response to immunological stress,
507 trauma and surgery (52). At the site of injury/trauma, pro-inflammatory cytokines are normally
508 released, activating inflammatory cells, ultimately resulting in inflammatory mediators and cytokines
509 being released into the extracellular fluid compartment to be circulated within the blood (52).

510 Interestingly, previous bioinformatic analyses of the proteome of late OA compared to healthy
511 controls, highlighted dysregulated acute phase response in the end-stage OA cohort (18). The
512 exacerbated activation of the acute phase response in non-responders following initial surgery could
513 indicate that these patients have a greater immune response to surgery and that they have a lesser
514 ability to dampen down the acute phase following surgery or that they have already developed an
515 advanced OA phenotype, deeming a therapy to repair cartilage injury unsuitable.

516 ~~Analysis of the canonical pathways which are associated with protein differences identified by either~~
517 ~~the iTRAQ nLC-MS/MS or the LF LC-MS/MS independently (1), highlighted many of the same~~
518 ~~biological pathways as being differentially regulated in response to cartilage harvest. Therefore,~~
519 ~~despite different proteins having been identified by the two methods, when these are considered~~
520 ~~alongside their likely interacting proteins in a 'systemic' manner, many common functional pathways~~
521 ~~have been identified irrespective of whole proteome coverage. Moreover, the overlap of biological~~
522 ~~pathways identified when comparing iTRAQ nLC-MS/MS and LF LC-MS/MS analyses adds~~
523 ~~confidence to our assertion that the biological mechanisms identified as underlying ACI success or~~
524 ~~failure warrant further investigation.~~

525 Finally, the datasets of combined iTRAQ nLC-MS/MS and LF LC-MS/MS identified proteins were
526 used to generate interactome models that represent the systemic proteome response to cartilage
527 harvest that exists within the SF of both ACI responders and non-responders, from which biological
528 functional pathways could be further studied. Biological functional pathways that were identified using
529 this approach, as well as using IPA can most confidently be taken forward as candidates for further
530 study, as they have been identified by independent bioinformatic methods. Furthermore, given the
531 complexity of the knee joint environment, it is likely that the responder/non-responder phenotype is
532 the result of many subtle protein changes which together contribute to overall dysfunction of a
533 biological network, rather than the result of an individual biological molecule or pathway *per se*.
534 Therefore, the interactome models generated in this study provide an important opportunity to
535 consider how these proteins interact with one another and result in such phenotypes, as well as,
536 providing a platform for further studies to investigate how potential modifications to the ACI procedure
537 e.g. using co-incidental anti-inflammatory drugs in non-responders at Stage II, may alter these

538 biological networks. Thus, these models may provide a potential *in silico* tool for predicting ACI
539 outcome, as is commonly used in drug development strategies (53).

540 **Conclusion**

541 This study has highlighted the advantage of using two independent proteomic techniques to profile a
542 holistic overview of the SF proteome, ideal for unbiased identification of biomarker candidates. iTRAQ
543 nLC-MS/MS analysis of SF samples from individuals who have either responded well or very poorly to
544 ACI has highlighted proteins that with further validation have the potential to predict clinical outcome
545 prior to treatment. We have confirmed that there is a marked SF proteome shift following cartilage
546 injury, which is exacerbated in non-responders. Network and pathway analyses have demonstrated
547 the complexity of the biological response underlying this proteome shift in non-responders, with
548 several biological pathways identified that may act as targets for therapeutic intervention.

549

550

551

552

553

554

555

556

557

558

559

560

561

562

563

564 **References**

- 565 1. Kraus VB, Blanco FJ, Englund M, Henrotin Y, Lohmander LS, Losina E, et al. OARSI Clinical
566 Trials Recommendations: Soluble biomarker assessments in clinical trials in osteoarthritis.
567 *Osteoarthr Cartil.* 2015;23(5):686–97.
- 568 2. National Institute for Health and Care Excellence. Autologous chondrocyte implantation for
569 treating symptomatic articular cartilage defects of the knee [Internet]. 2017. Available from:
570 [https://www.nice.org.uk/guidance/ta477/resources/autologous-chondrocyte-implantation-for-](https://www.nice.org.uk/guidance/ta477/resources/autologous-chondrocyte-implantation-for-treating-symptomatic-articular-cartilage-defects-of-the-knee-pdf-82604971061701)
571 [treating-symptomatic-articular-cartilage-defects-of-the-knee-pdf-82604971061701](https://www.nice.org.uk/guidance/ta477/resources/autologous-chondrocyte-implantation-for-treating-symptomatic-articular-cartilage-defects-of-the-knee-pdf-82604971061701)
- 572 3. Hulme CH, Wilson EL, Peffers MJ, Roberts S, Simpson DM, Richardson JB, et al. Autologous
573 chondrocyte implantation-derived synovial fluids display distinct responder and non-responder
574 profiles. *Arthritis Res Ther.* 2017;19:150.
- 575 4. Gillogly SD, Voight M, Blackburn T. Treatment of articular cartilage defects of the knee with
576 autologous chondrocyte implantation. *J Orthop Sport Phys Ther.* 1998;28(4):241–51.
- 577 5. Richardson JB, Caterson B, Evans EH, Ashton BA, Roberts S. Repair of human articular
578 cartilage after implantation of autologous chondrocytes. *J Bone Joint Surg Br.*
579 1999;81(6):1064–8.
- 580 6. Wright KT, Mennan C, Fox H, Richardson JB, Banerjee R, Roberts S. Characterization of the
581 cells in repair tissue following autologous chondrocyte implantation in mankind: a novel report
582 of two cases. *Regen Med.* 2013;8:699–709.
- 583 7. Bhosale AM, Kuiper JH, Johnson WE, Harrison PE, Richardson JB. Midterm to long-term
584 longitudinal outcome of autologous chondrocyte implantation in the knee joint: a multilevel
585 analysis. *Am J Sports Med.* 2009;37(Suppl 1):131S – 8S.
- 586 8. Wright KT, Kuiper JH, Richardson JB, Gallacher P, Roberts S. The absence of detectable
587 ADAMTS-4 (aggrecanase-1) activity in synovial fluid is a predictive indicator of autologous
588 chondrocyte implantation success. *Am J Sports Med.* 2017;45(8):1806–14.
- 589 9. Dugard MN, Herman Kuiper J, Parker J, Roberts S, Robinson E, Harrison P, et al.
590 Development of a Tool to Predict Outcome of Autologous Chondrocyte Implantation. *Cartilage.*
591 2016;1–12.
- 592 10. Hsueh MF, Onnerfjord P, Kraus VB. Biomarkers and proteomic analysis of osteoarthritis.
593 *Matrix Biol.* Elsevier B.V.; 2014;39:56–66.
- 594 11. Chiaradia E, Pepe M, Tartaglia M, Scoppetta F, D'Ambrosio C, Renzone G, et al. Gambling on
595 putative biomarkers of osteoarthritis and osteochondrosis by equine synovial fluid proteomics.
596 *J Proteomics.* 2012;75:4478–93.
- 597 12. Pan X, Huang L, Chen J, Dai Y, Chen X. Analysis of synovial fluid in knee joint of
598 osteoarthritis: 5 Proteome patterns of joint inflammation based on matrix-assisted laser
599 desorption/ionization time-of-flight mass spectrometry. *Int Orthop.* 2012;36(1):57–64.
- 600 13. Sohn DH, Sokolove J, Sharpe O, Erhart JC, Chandra PE, Lahey LJ, et al. Plasma proteins
601 present in osteoarthritic synovial fluid can stimulate production via Toll-like receptor 4. *Arthritis*
602 *Res Ther.* 2012;14(1):R7.
- 603 14. Liao W, Li Z, Wang H, Wang J, Fu Y, Bai X. Proteomic analysis of synovial fluid: Insight into
604 the pathogenesis of knee osteoarthritis. *Int Orthop.* 2013;37(6):1045–53.

- 605 15. Noh R, Park SG, Ju JH, Chi SW, Kim S, Lee CK, et al. Comparative proteomic analyses of
606 synovial fluids and serums from rheumatoid arthritis patients. *J Microbiol Biotechnol.*
607 2014;24(1):119–26.
- 608 16. Liao W, Li Z, Zhang H, Li J, Wang K, Yang Y. Proteomic analysis of synovial fluid as an
609 analytical tool to detect candidate biomarkers for knee osteoarthritis. *Int J Clin Exp Pathol.*
610 2015;8(9):9975–89.
- 611 17. Mateos J, Lourido L, Fernández-Puente, P Calamia V, Fernández-López, C Oreiro N, Ruiz-
612 Romero C, Blanco FJ. Differential protein profiling of synovial fluid from rheumatoid arthritis
613 and osteoarthritis patients using LC–MALDI TOF/TOF. *J Proteomics.* 2012;75(10):2869–78.
- 614 18. Ritter SY, Subbaiah R, Bebek G, Crish J, Scanzello CR, Krastins B, et al. Proteomic analysis
615 of synovial fluid from the osteoarthritic knee: Comparison with transcriptome analyses of joint
616 tissues. *Arthritis Rheum.* 2013;65(4):981–92.
- 617 19. Balakrishnan L, Nirujogi RS, Ahmad S, Bhattacharjee M, Manda SS, Renuse S, et al.
618 Proteomic analysis of human osteoarthritis synovial fluid. *Clin Proteomics.* 2014;11(1):1–13.
- 619 20. Balakrishnan L, Bhattacharjee M, Ahmad S, Nirujogi RS, Renuse S, Subbannayya Y, et al.
620 Differential proteomic analysis of synovial fluid from rheumatoid arthritis and osteoarthritis
621 patients. *Clin Proteomics.* 2014;11(1):1.
- 622 21. Bennike T, Ayturk U, Haslauer CM, Froehlich JW, Proffen BL, Barnaby O, et al. A normative
623 study of the synovial fluid proteome from healthy porcine knee joints. *J Proteome Res.*
624 2014;13(10):4377–87.
- 625 22. Bhattacharjee M, Balakrishnan L, Renuse S, Advani J, Goel R, Sathe G, et al. Synovial fluid
626 proteome in rheumatoid arthritis. *Clin Proteomics.* BioMed Central; 2016;1–11.
- 627 23. Wu WW, Wang G, Baek SJ, Shen RF. Comparative study of three proteomic quantitative
628 methods, DIGE, cICAT, and iTRAQ, using 2D gel- or LC-MALDI TOF/TOF. *J Proteome Res.*
629 2006;5(3):651–8.
- 630 24. Bantscheff M, Schirle M, Sweetman G, Rick J, Kuster B. Quantitative mass spectrometry in
631 proteomics: a critical review. *Anal Bioanal Chem.* 2007;389(4):1017–31.
- 632 25. Lilley KS, Beynon RJ, Eyers CE, Hubbard SJ. Focus of Quantitative Proteomics. *Proteomics.*
633 2015;15(18):3101–3.
- 634 26. Herr MM, Fries KM, Upton LG, Edsberg LE. Potential biomarkers of temporomandibular joint
635 disorders. *J Oral Maxillofac Surg.* 2011;69(1):41–7.
- 636 27. Roberts S, Evans H, Wright K, van Niekerk L, Caterson B, Richardson JB, et al. ADAMTS-4
637 activity in synovial fluid as a biomarker of inflammation and effusion. *Osteoarthritis Cartilage.*
638 2015;23(9):1622–6.
- 639 28. Kraus V, Stabler T, Kong S, Varjum G, McDaniel G. Measurement of synovial fluid volume
640 using urea. *Osteoarthr Cartil.* 2007;15(1217):e20.
- 641 29. Ehrich E, Davies G, Watson D, Bolohnese J, Seidenberg B, Bellamy N. Minimal perceptible
642 clinical improvement with the Western Ontario and McMaster Universities osteoarthritis index
643 questionnaire and global assessments in patients with osteoarthritis. *J Rheumatol.*
644 2000;27(11):2635–41.
- 645 30. Roos E, Lohmander L. The Knee Injury and Osteoarthritis Outcome Score (KOOS): from joint
646 injury to osteoarthritis. *Health Qual Life Outcomes.* 2003;1:64.
- 647 31. Saris D, Vanlauwe J, Victor J, Almqvist K, Verdonk R, Bellemans J, et al. Treatment of
648 symptomatic cartilage defects in the knee: characterized chondrocyte implantation results in
649 better clinical outcome at 36 months in a randomized trial compared to microfracture. *Am J*
650 *Sports Med.* 2009;37(Suppl 1):10S – 19S.

- 651 32. Smith H, Richardson J, Tennant A. Modification and validation of the Lysholm Knee Scale to
652 assess articular cartilage damage. *Osteoarthr Cartil.* 2009;17:55–8.
- 653 33. Lysholm J, Gillquist J. Evaluation of knee ligament surgery results with special emphasis on
654 use of a scoring scale. *Am J Sports Med.* 1982;10(3):150–4.
- 655 34. Stoscheck CM. Protein assay sensitive at nanogram levels. *Anal Biochem.* 1987;160(2):301–
656 5.
- 657 35. Fuller HR, Mandefro B, Shirran SL, Gross AR, Kaus A, Botting CH, et al. Spinal muscular
658 atrophy patient iPSC-derived motor neurons have reduced expression of proteins important in
659 neuronal development. *Front Cell Neurosci.* 2016;9(506).
- 660 36. Fuller H, Slade R, Jovanov-Milošević N, Babić M, Sedmak G, Šimić G, et al. Stathmin is
661 enriched in the developing corticospinal tract. *Mol Cell Neurosci.* 2015;12(69):12–21.
- 662 37. Oliveros JC. VENNY. An interactive tool for comparing lists with Venn Diagrams. BioinfoGP of
663 CNB-CSIC. 2007. p. <http://bioinfogp.cnb.csic.es/tools/venny/index.ht>.
- 664 38. Albert R, Barabasi AL. Statistical mechanics of complex networks. *Rev Mod Phys.*
665 2002;74(1):47–97.
- 666 39. Vidal M, Cusick ME, Barabási A-L. Interactome networks and human disease. *Cell.* *Cell Press;*
667 2011;144(6):986–98.
- 668 40. Cowley MJ, Pinese M, Kassahn KS, Waddell N, Pearson J V., Grimmond SM, et al. PINA v2.0:
669 Mining interactome modules. *Nucleic Acids Res.* 2012;40(D1):862–5.
- 670 41. Barabási A-L, Gulbahce N, Loscalzo J. Network medicine: a network-based approach to
671 human disease. *Nat Rev Genet.* 2011;12(1):56–68.
- 672 42. Nepusz T, Yu H, Paccanaro A. Detecting overlapping protein complexes in protein-protein
673 interaction networks. *Nature Methods.* 2012. p. 471–2.
- 674 43. Reactome. Reactome - a curated knowledgebase of biological pathways. *Genome Biology.*
675 2008. p. R39.
- 676 44. Croft D, Mundo AF, Haw R, Milacic M, Weiser J, Wu G, et al. The Reactome pathway
677 knowledgebase. *Nucleic Acids Res.* 2014;42(Database issue):D472–7.
- 678 45. Clemmons DR, Busby WH, Garmong A, Schultz DR, Howell DS, Altman RD, et al. Inhibition of
679 Insulin-Like Growth Factor Binding Protein 5 Proteolysis in Articular Cartilage and Joint Fluid
680 Results in Enhanced Concentrations of Insulin-Like Growth Factor 1 and Is Associated With
681 Improved Osteoarthritis. *Arthritis Rheum.* 2002;46(3):694–703.
- 682 46. Busby WH, Yocum SA, Rowland M, Kellner D, Lazerwith S, Sverdrup F, et al. Complement 1s
683 is the Serine Protease that Cleaves IGFBP-5 in Human Osteoarthritic Joint Fluid. *Osteoarthr*
684 *Cartil.* 2009;17(4):547–55.
- 685 47. van Osch GJVM, van den Berg WB, Hunziker EB, Hauselmann HJ. Differential effects of IGF-
686 1 and TGF beta-2 on the assembly of proteoglycans in pericellular and territorial matrix by
687 cultured bovine articular chondrocytes. *Osteoarthr Cartil.* 1998;6:187–95.
- 688 48. Wang Q, Rozelle AL, Lepus CM, Scanzello CR, Song JJ, Larsen DM, et al. Identification of a
689 central role for complement in osteoarthritis. *Nat Med.* 2012;17(12):1674–9.
- 690 49. Murphy G. Matrix metalloproteinases and their inhibitors. *Acta Orthop Scand Suppl.*
691 1995;266:55–60.
- 692 50. Wakitani S, Imoto K, Yamamoto T, Saito M, Murata N, Yoneda M. Human autologous culture
693 expanded bone marrow mesenchymal cell transplantation for repair of cartilage defects in
694 osteoarthritic knees. *Osteoarthr Cartil.* 2002;10(3):199–206.

- 695 51. Wakitant S, Okabe T, Horibe S, Mitsuoka T, Saito M, Koyama T, et al. Safety of autologous
696 bone marrow-derived mesenchymal stem cell transplantation for cartilage repair in 41 patients
697 with 45 joints followed for up to 11 years and 5 months. *J Tissue Eng Regen Med.*
698 2011;5(2):146–50.
- 699 52. Gruys E, Toussaint MJM, Niewold TA, Koopmans SJ. Acute phase reaction and acute phase
700 proteins. *J Zhejiang Univ Sci B.* 2005;6(11):1045–56.
- 701 53. Guney E, Menchem J, Vidal M, Barabasi A-L. Network-based in silico drug efficacy screening.
702 *Nat Commun.* 2016;7:10331.

703

704

705

706

707

708

709

710

711

712

713

714

715

716

717

718

719

720

721

722

723

724

725

726

727

728

729

730

731

732

733 **List of Abbreviations**

734 ACI, autologous chondrocyte implantation; BMI, body mass index; C1s, Complement 1S
735 subcomponent; iTRAQ, isobaric tagging for relative and absolute quantitation; LC-MS/MS, liquid
736 chromatography- tandem mass spectrometry; LF, label-free quantitation; LFC, lateral femoral
737 condyle; LTP, lateral tibial plateau; MFC, medial femoral condyle; LXR/RXR, Liver X receptor/
738 Retinoic X receptor; MMP3, matrix metalloproteinase 3; nLC-MS/MS, nano liquid chromatography-
739 tandem mass spectrometry; NICE, The National Institute for Health and Care Excellence; NHS,
740 National Health Service OA, osteoarthritis; OARSI, Osteoarthritis Research Society International;
741 PINA4MS, Protein Interaction Network Analysis For Multiple Sets; SF, synovial fluid; SRC, proto-
742 oncogene tyrosine-protein kinase; TEAB, triethylammonium bicarbonate; TGFB1, transforming growth
743 factor beta 1

744 **Declarations**

745 Ethics approval and consent to participate

746 SF samples from patients undergoing ACI were collected under three independent ethical approvals:
747 'Investigating the potential for cells and molecules isolated from orthopaedic patients for modelling
748 and understanding pathogenic conditions and developing diagnostic markers and therapies for
749 musculoskeletal disorders and spinal cord injury' (11/NW/0875); 'Autologous cell therapy for
750 Osteoarthritis: An evaluation of the safety and efficacy of autologous transplantation of articular
751 chondrocytes and/or bone marrow derived stromal cells to repair chondral/osteochondral lesions of
752 the knee' (11/WM/0175) and 'Arthritis and cartilage repair study' (06/Q6201/9). 11/NW/0875 was
753 approved by the NRES committee North West- Liverpool East. 11/WM/0175 was approved by the
754 NRES committee West Midlands - Coventry and Warwick and 06/Q2601/9 was approved by
755 Shropshire and Staffordshire-Shropshire local research ethics committee. All patients gave valid
756 informed consent prior to samples being collected.

757 Consent for publication

758 Not applicable for this study.

759 Availability of data and material

760 Proteomic data has been deposited in the PRIDE ProteomeXchange and can be accessed using the
761 identifier PXD008321.

762 Competing interests

763 The authors declare that they have no competing interests.

764 Funding

765 We would like to thank Arthritis Research UK for supporting this work via grants 19429, 20815 and
766 21122. The sponsors had no involvement in the study design, data collection and interpretation or
767 preparation of the manuscript. Mandy Peffers is supported through a Wellcome Trust Clinical
768 Intermediate Fellowship. This work was supported by the Wellcome Trust grant 094476/Z/10/Z which
769 funded the purchase of the TripleTOF 5600 mass spectrometer at the BSRC Mass Spectrometry and
770 Proteomics Facility, University of St Andrews.

771 Authors' contributions

772 CHH, ELW, KTW, HRF, MJP & SR came up with conception and design of the study. CHH, ELW,
773 HRJ, SLS & CHB collected data which was then analysed and interpreted by CHH, ELW, KTW, MJP
774 & HRF. CHH, ELW, HRF, SR, MJP, SLS, CHB, JBR, PG & KTW drafted the manuscript, critically
775 revised and approved the final article. PG & JBR provided patients' synovial fluid samples. Funding
776 for the study was obtained by KTW & SR. All authors read and approved the final manuscript.

777 Acknowledgments

778 We would like to thank Professor Rob Beynon for his advice on study design and help with analysis of
779 samples using label free quantitation proteomic analysis.

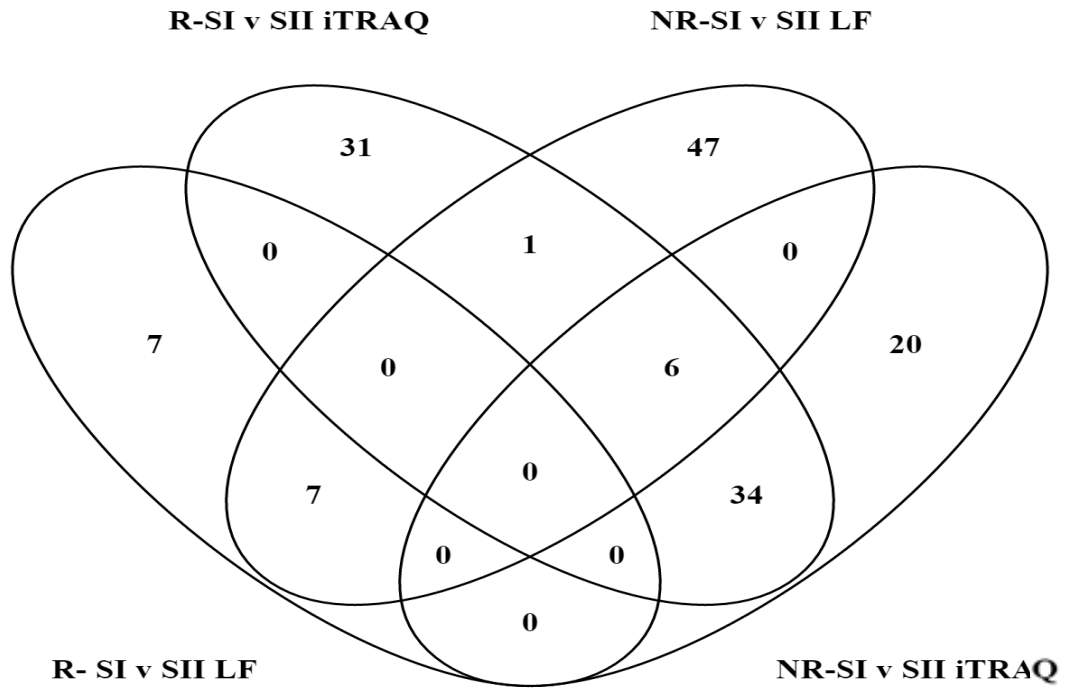
780

781

782

783

784



785 **Figure 1:** Venn-Diagrams representing the proteins identified using isobaric tags for relative and absolute
786 quantitation (iTRAQ) proteomics and label-free quantitation (LF) proteomics which were differentially
787 abundant (≥ 2.0 FC; $p \leq 0.05$) in the SF at Stage I (SI) compared to Stage II (SII) in responders (R) compared to
788 non-responders (NR) to ACI.

789

790

791

792

793

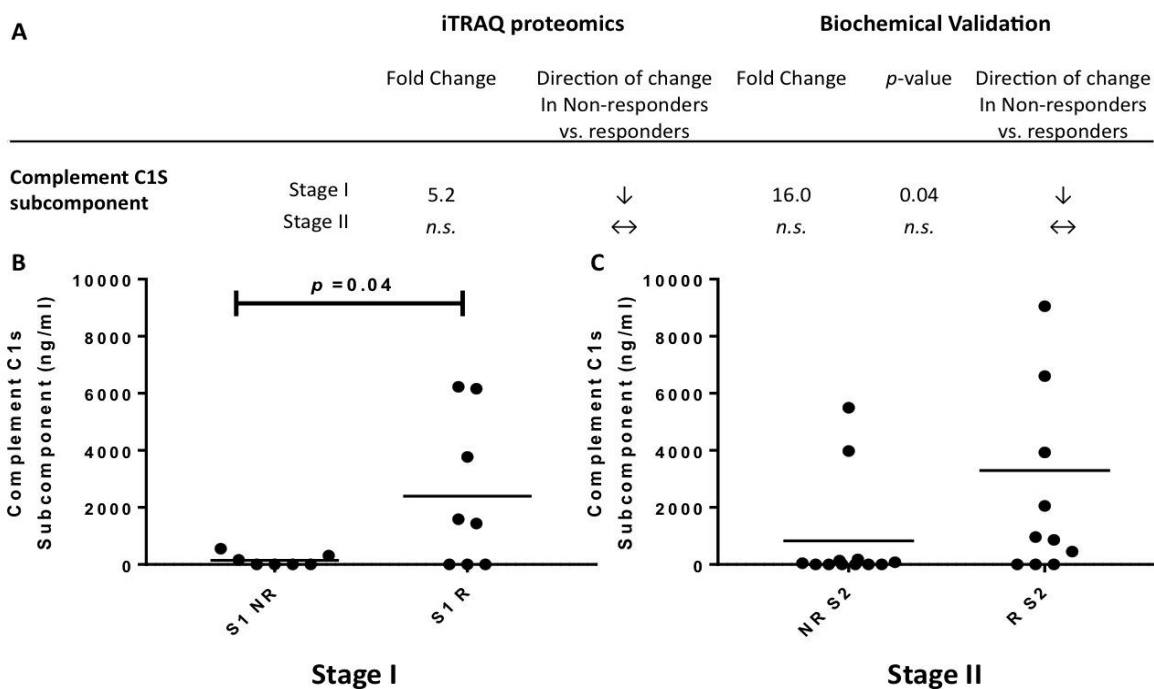
794

795

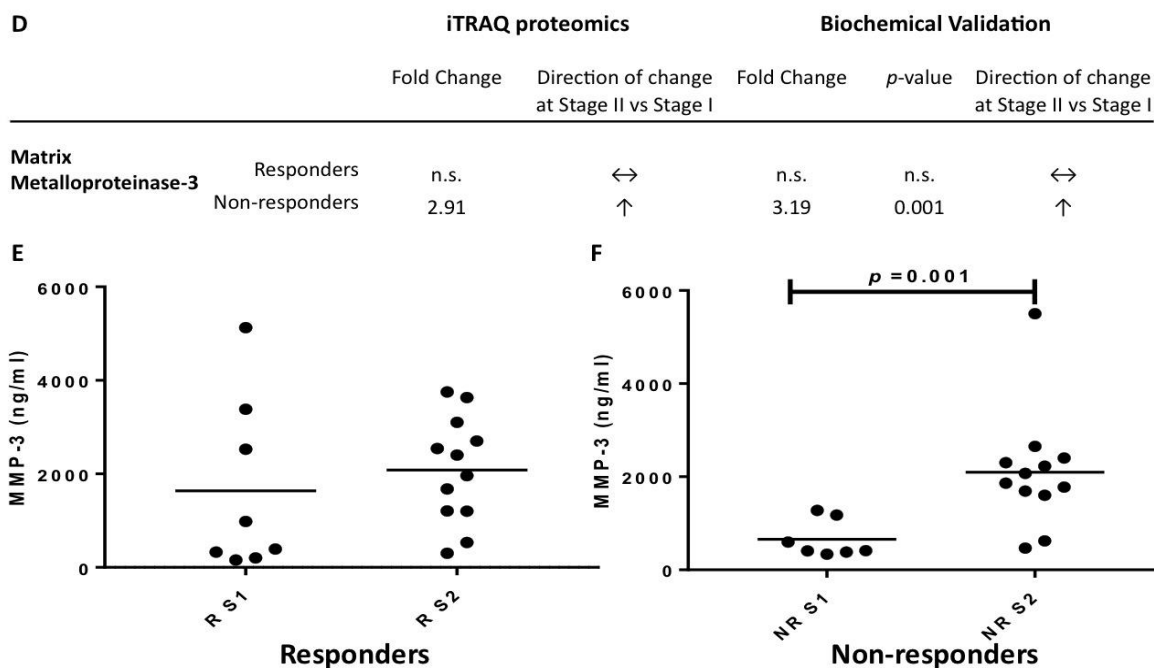
796

797

Complement C1S Subcomponent



Matrix Metalloproteinase-3



798 **Figure 2: Biochemical validation of differentially abundant proteins identified using isobaric tagging for**
 799 **relative and absolute quantitation (iTRAQ) proteomics. (A) and (D) demonstrate the differential abundance of**
 800 **Complement C1S subcomponent and Matrix metalloproteinase-2, respectively as measured by iTRAQ mass-**
 801 **spectrometry and by biochemical ELISA. Quantitative ELISA confirmed that (B) Complement C1S**
 802 **subcomponent is significantly decreased in the synovial fluid (SF) of non-responders (NR) compared to**
 803 **responders (R) to Autologous Chondrocyte Implantation (ACI) prior to cartilage harvest (Stage I; S1; $p=0.04$;**
 804 **Student's *t*-test)(C) but was not significantly differentially abundant prior to chondrocyte implantation (Stage**
 805 **II; S2). (E) Matrix metalloproteinase-3 (MMP3) is not differentially abundant in response to cartilage harvest in**
 806 **ACI responders (F) but was biochemically confirmed to be differentially abundant in the SF of non-responders**
 807 **between Stages I and II of the ACI procedure ($p=0.001$; Student's *t*-test).**

808

809

810

811

812

813

814

815

816

817

818

819

820

821

822

823

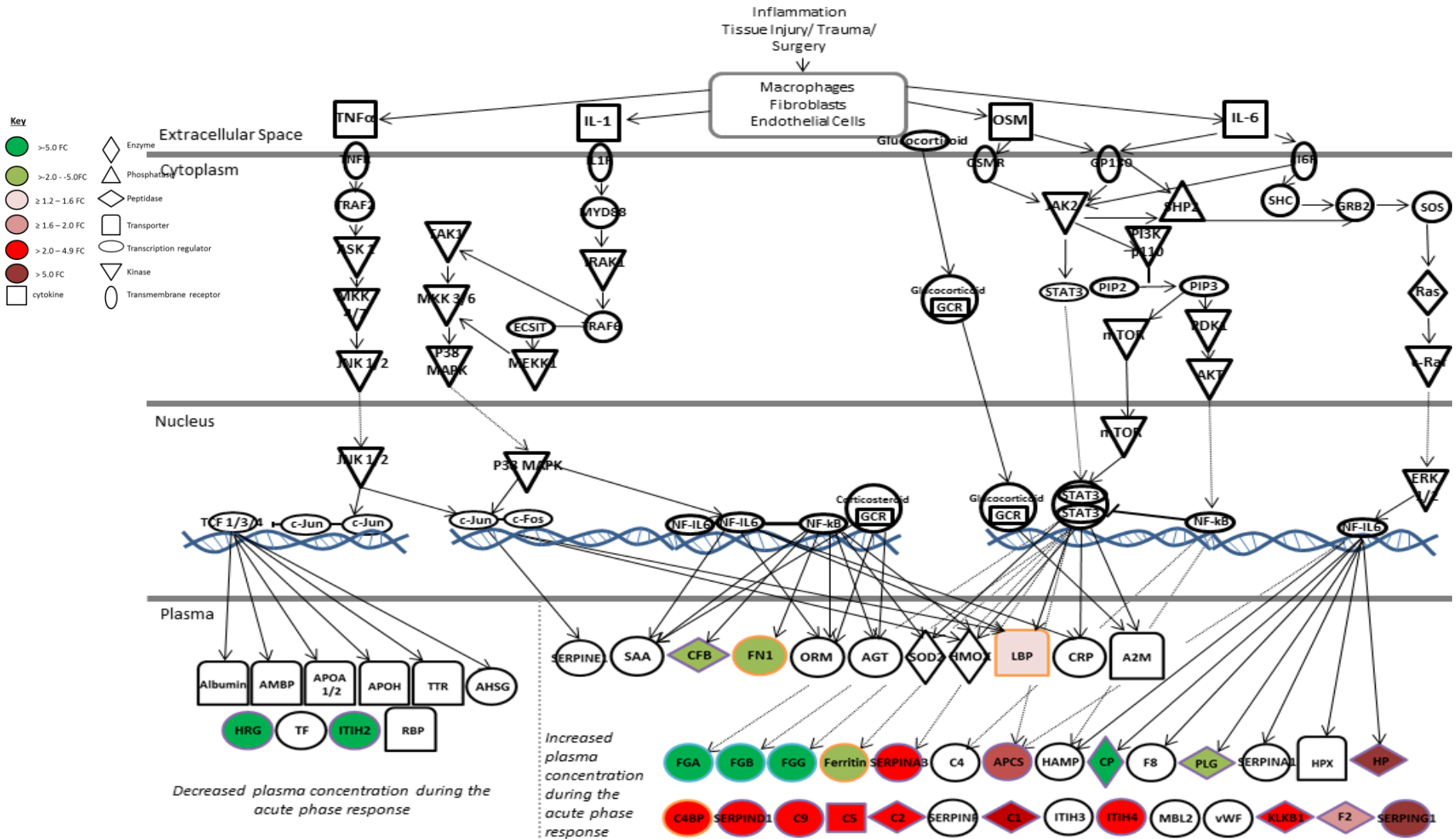
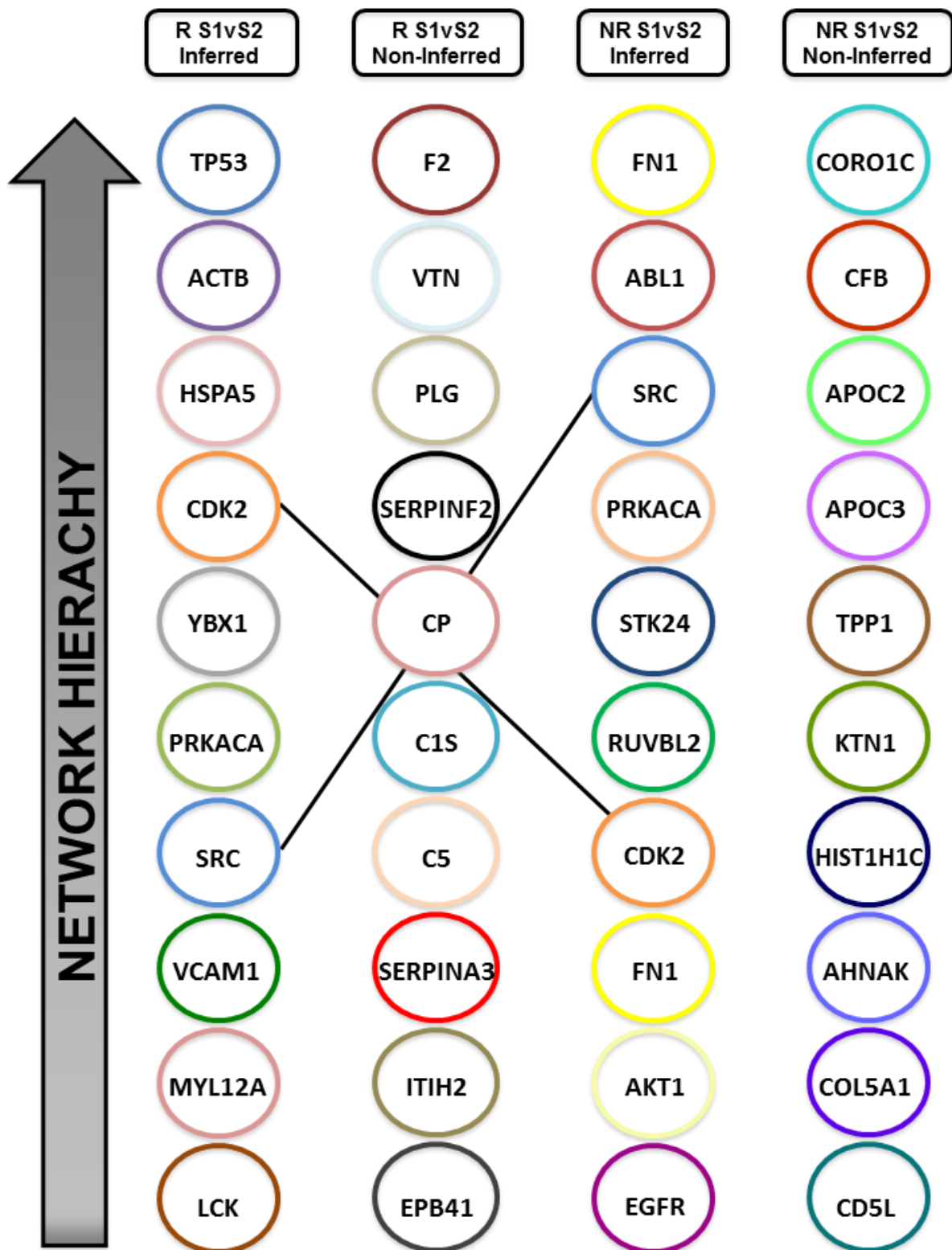


Figure 3: Proteins of Acute Phase Signalling at Stage II compared to Stage I in non-responders to Autologous Chondrocyte Implantation (ACI). Several synovial fluid proteins that are downstream of acute phase response signalling were differentially abundant between Stages I and II of ACI. Proteins edged in purple, orange and blue were identified using iTRAQ nLC-MS/MS, LF LC-MS/MS or by both techniques, respectively. (Adapted from Ingenuity).



824

825 **Figure 4: The ModuLand algorithm was applied to inferred and non-inferred interactome networks of**
 826 **differentially abundant proteins ($\pm 1.2FC$; $p \leq 0.05$) between Stages I and II of ACI in clinical responders and**
 827 **non-responders. Modules were identified from both non-inferred (protein changes identified from proteomic**
 828 **analysis only) and inferred (identified protein changes and inferred proteins interactions) networks and are**
 829 **ranked based on their hierarchical network connectivity.**

